Alkaline-Earth-Metal Antimonides and Bismuthides with the A_5Pn_3 Stoichiometry. Interstitial and Other Zintl Phases Formed on Their Reactions with Halogen or Sulfur

Weir-Mirn Hurng and John D. Corbett*

Ames Laboratory—DOE[1] and the Department of Chemistry, Iowa State University, Ames, Iowa 50011

Received December 16, 1988

The phase A_5Pn_3 (A = Ca, Sr, or Ba; Pn = Sb or Bi) have been synthesized in high yield in welded Ta containers and confirmed to have either the Mn_5Si_3 (M) or the β-Yb_5Sb_3 (Y) structure types, or both. Lattice constants from Guinier powder diffraction suggest most previous reports on these phases probably pertained to binary compounds. These phases in the presence of chlorine or, where attempted, bromine form Zintl phases A_5Pn_3X (X = Cl, Br) in the same M structure but with halogen in all octahedral cavities of the confacial $A_{6/2}Pn_{6/2}$ chains. Two chlorides were studied by single-crystal means (space group $P6_3/mcm$; Ca_5Sb_3Cl: a = 9.0805 (3) Å, c = 7.0898 (6) Å, R/R_w = 3.8/5.9%; Ba_5Sb_3Cl: a = 10.062 (4) Å, c = 7.770 (6) Å, 5.1/8.9%). X-ray study of single-crystal Sr_5Sb_3 in the same structure type confirmed the stoichiometry and the absence of atoms in the interstitial cavity (a = 9.5037 (5) Å, c = 7.4095 (8) Å, 3.2/2.9%). The M-type analogues Ce_5Sb_3Cl, Ce_5Bi_3Cl, and Ce_5Bi_3Br also form readily. Fluorine reacts with Ca_5Sb_3 and Ca_5Bi_3 but not Ba_5Sb_3 to form Y-type structure analogues with fluoride in a suitable tetrahedral cavity (space group $Pnma$; Ca_5Sb_3F: a = 12.442 (2) Å, b = 9.653 (2) Å, c = 8.381 (2) Å, R/R_w = 2.5/3.3; Ca_5Bi_3F: a = 12.602 (2) Å, b = 9.771 (2) Å, c = 8.501 (2) Å, 6.0/5.8%). Reactions of Ca_5Sb_3 with the appropriate proportions of C, O, or S yield CaC_2, the known Ca_4Sb_2O, or the new valence compound $Ba_4Sb_{2.4}S_{0.4}$ in a defect, anti-Th_3P_4 type structure (a = 9.6508 (3) Å). Iodine with Ba_5Sb_3 analogously yields a 2:1 proportion of $Ba_4Sb_{2.5}I_{0.5}$ (anti-Th_3P_4, $I\bar{4}3d$, a = 10.475 (7) Å, R/R_w = 8.8/10.0%) and Ba_2SbI (disordered NaCl, a = 7.0970 (6) Å).

Introduction

Literature reports on the A_5Pn_3 compounds that form between alkaline-earth elements (A = Ca, Sr, Ba) and the heavier pnictides (Pn = As, Sb, Bi) leave several uncertainties regarding both their structures and compositions. The majority have been found to have the hexagonal Mn_5Si_3 structure, namely, all three arsenides,[2] Ca_5Sb_3,[3] Sr_5Sb_3,[4] Sr_5Bi_3, Ba_5Sb_3,[5] and Ba_5Bi_3.[3,5] In addition, a different β-Yb_5Sb_3 (orthorhombic) structure type has been reported for Ca_5Sb_3,[6] Ca_5Bi_3,[7] and Sr_5Bi_3.[3] In neither case were both polymorphs of Ca_5Sb_3 or Sr_5Bi_3 seen in the initial study.

The prominence of the Mn_5Si_3 structure type among these phases gives reason for caution since many other compounds with this structure are known to bind a third element interstitially to give A_5Pn_3Z phases or perhaps even to *require* such for stability.[8-11] We will also show that fluoride can be bonded analogously in examples of the second, β-Yb_5Sb_3-type structure. Furthermore, all prior single-crystal studies of these A_5Pn_3 phases[2,4-7] appear to leave the possible presence of a third "interstitial" element unresolved since in no case did the authors note that a Fourier or difference Fourier map had been examined for a possible impurity component. These reports also did not make clear whether the A_5Pn_3 phases were obtained as major or incidental products, a characteristic that can provide an important diagnosis regarding possible impurity stabilization.[12]

Phases with an A_2Pn composition in the La_2Sb structure were also seen in many of these studies, materials that have later been concluded to actually be valence (Zintl) compounds A_4Pn_2O (anti-K_2NiF_4 type) based on the examples of Ca_4Sb_2O[13] and Eu_4As_2O.[14] An analogous possibility for the same group of A_5Pn_3 compounds has also been suggested,[15] viz., $A_{10}Pn_6O$, presumably either with disordered oxygen or in some sort of superstructure. But the possibility that halide interstitials might occur in isostructural Zintl phases A_5Pn_3X of either structure type has evidently not been considered. Such impurities could have been a significant source of minor products in the previous efforts since alkaline-earth metals are commonly prepared by electrolysis of their chlorides, and these sometimes have also been consolidated by fusing them under a chloride flux.[16]

The present investigation undertook to clarify, first, whether the alkaline-earth-metal antimonides and bismuthides reported earlier were binary phases or not. For this purpose, their syntheses were carried out from high-purity elements and, whenever possible, so as to give single-phase products. A single-crystal structural analysis for the Mn_5Si_3 type of one of the dimorphic examples, Sr_5Sb_3, was also performed to establish whether the potential in-

(1) The Ames Laboratory-DOE is operated for the U. S. Department of Energy by Iowa State University under Contract No. W-7405-Eng-82. This research was supported by the Office of Basic Energy Sciences, Materials Sciences Division.

(2) Better, B.; Hütz, A.; Nagorsen, G. *Z. Metallkd.* **1976**, *67*, 118.
(3) Bruzzone, G.; Franceschi, E.; Merlo, F. *J. Less-Common Met.* **1978**, *60*, 59.
(4) Martinez-Ripoll, M.; Brauer, G. *Acta Crystallogr.* **1973**, *B29*, 2717.
(5) Eisenmann, B.; Deller, K. *Z. Naturforsch.* **1975**, *30b*, 66.
(6) Martinez-Ripoll, M.; Brauer, G. *Acta Crystallogr.* **1974**, *B30*, 1083.
(7) Martinez-Ripoll, M.; Haase, A. Brauer, G. *Acta Crystallogr.* **1974**, *B30*, 2004.
(8) Rossteutscher, W.; Schubert, K. *Z. Metallkd.* **1965**, *56*, 813.
(9) Nowotny, H.; Benesovsky, F. In *Phase Stability in Metals and Alloys*; Rudman, P. S., Stringer, J., Jaffee, R. I., Eds.; McGraw-Hill: New York, 1966; p 319.
(10) Garcia, E.; Corbett, J. D. *Inorg. Chem.* **1988**, *27*, 2907.
(11) Corbett, J. D.; Garcia, E.; Kwon, Y.-U.; Guloy, A. *Pure Appl. Chem.*, in press.
(12) Rosenthal, G.; Corbett, J. D. *Inorg. Chem.* **1988**, *27*, 53.
(13) Eisenmann, B.; Limartha, H.; Schafer, H.; Graf, H. A. *Z. Naturforsch.* **1980**, *35b*, 1518.
(14) Taylor, J. B.; Calvert, L. D.; Utsunomiya, T.; Wang, Y.; Despault, J.-G. *J. Less-Common Met.* **1978**, *57*, 39.
(15) Schafer, H.; Eisenmann, B. *Rev. Inorg. Chem.* **1981**, *3*, 29.
(16) Peterson, D. T., private communication.

0897-4756/89/2801-0311$01.50/0

Table I. Diffraction and Refinement Data[a]

	Sr_5Sb_3	Ca_5Sb_3Cl	Ba_5Sb_3Cl	Ca_5Sb_3F	Ca_5Bi_3F	$Ba_4Sb_{2.5}I_{0.5}$
space group	$P6_3/mcm$ (No. 192)	$P6_3/mcm$	$P6_3/mcm$	$Pnma$ (No. 62)	$Pnma$	$I\bar{4}3d$
Z	2	2	2	4	4	4
cell param,[b] Å						
a	9.5037 (5)	9.0805 (3)	10.062 (4)	12.442 (2)	12.602 (2)	10.475 (7)
b	a	a	a	9.653 (2)	9.771 (2)	
c	7.4095 (8)	7.0898 (6)	7.770 (6)	8.381 (2)	8.501 (2)	
cryst size, mm	0.08 × 0.15 × 0.12	0.08 × 0.08 × 0.08	0.10 × 0.10 × 0.10	0.23 × 0.18 × 0.10	0.13 × 0.18 × 0.03	0.15 × 0.12 × 0.08
octants coll	$h,k,\pm l$	$h,k,\pm l$	$h,k,\pm l$	$\pm h,\pm k,l$	$\pm h,\pm k,l$	$\pm h,\pm k,l$
2θ(max), deg	55	50	50	55	55	55
μ(Mo Kα), cm^{-1}	292.5	105.8	206.6	105.3	530.1	205.0
transm coeff range	0.23–0.43	0.32–1.00[c]	0.52–1.00[c]	0.15–0.17	0.05–0.40	0.35–0.47
reflctns						
measd	928	737	945	2386	2072	722
obsd ($>3\sigma(I)$)	825	571	756	2147	1769	653
indep	251	190	248	1127	899	197
R(av)	0.024	0.035	0.028	0.019	0.037	0.030
R^d	0.032	0.038	0.051	0.025	0.060	0.088
R_w[d]	0.029	0.059	0.089	0.033	0.058	0.100
interst occ		1.00 (4)	1.10 (6)	1.01 (1)	0.97 (5)	
sec extin coeff ($\times 10^5$)	0.47 (7)			5.5 (2)		

[a] Mo Kα radiation and ω-scan in all cases. [b] Cell dimensions from Guinier measurements. [c] Normalized. [d] $R = \sum||F_o| - |F_c||/\sum|F_o|$, $R_w = [\sum w(|F_o| - |F_c|)^2/\sum w|F_o|^2]^{1/2}$.

terstitial site was indeed empty. This seemed desirable since $Sr_5Sb_{3.33}$ with self-interstitials, structurally analogous to Zr_5Sb_{3+x},[17] would also be a Zintl phase. The A_5Pn_3 or other structures obtained when syntheses of selected A_5Pn_3 phases are carried out in the presence, effectively, of each of the halogens, carbon, oxygen, or sulfur (Z) are also described. Finally, the lattice dimensions for these A_5Pn_3 and A_5Pn_3Z compounds obtained by Guinier powder methods are compared with literature data to see whether the nature of the products reported earlier might be judged on this basis.

Experimental Section

Synthesis. The studies were carried out as before using conventional high-vacuum and glovebox techniques coupled with reactions in sealed Ta containers.[18] The box atmosphere was maintained at 1–5 ppm H_2O by volume by circulation through a bed of molecular sieve pellets. Although oxygen levels were not measured, the atmosphere was also circulated through a bed of Ridox (Fisher Scientific), and a 60-W light bulb without glass would customarily burn for 30–50 min before failure.

The alkaline-earth metals utilized had been distilled under high vacuum in the Ames Lab and were stored in the glovebox in screw-top containers. These typically contained other alkaline-earth-metal impurities as follows, in wt ppm, Ca: Sr 300, Ba 50; Sr: Ca 490, Ba 760; Ba: Ca 350 Sr 215. The C, N, and O contents after sublimation were estimated to be <100 ppm each. The Ca and Ba samples remained shiny under these storage conditions, while the older Sr sample was scraped free of any contamination as far as possible just before use. A rod form of Sr (AESAR) also used revealed a shiny surface after a layer of oxide was peeled off. The Yb employed in a few experiments was also a high-purity Ames Lab product. Characterization of the reagent-grade Sb used has been described before,[17] while the Bi was reactor grade (Oak Ridge National Lab). The components were weighed within the glovebox to ~1 mg and contained within a crimped Ta tube container prior to welding. The typical reaction scale was a few hundred milligrams.

Sources of interstitial chloride or bromide were the corresponding alkaline-earth-metal halides (reagent grade; Fisher, Baker, or ROC/RIC) that had been dried by slowly heating samples under high vacuum to 200–400 °C. These and other compounds used were then stored in sealed ampules or in stoppered vials within the glovebox. SbI_3 and $BiBr_3$ were made by reaction of the elements in stoichiometric amounts within a sealed fused silica apparatus at ~750 °C. BaF_2 was prepared by reaction of $BaCO_3$ (ACS) with 35% HF(aq) followed by heating of the white precipitate in a high vacuum from room temperature to ~400 °C. The CaF_2 and CaO employed were commercial products (Fisher, ACS) and the carbon, a spectroscopic grade of powder (Union Carbide).

Reactions at temperatures up to 1100 °C were carried out in Marshall tube furnaces with the Ta container jacketed by a well-evacuated and sealed, fused silica envelope. Induction heating of the container in a high vacuum was used when higher temperatures were needed, with temperatures measured with the aid of an optical pyrometer. Generally, the components were first reacted by heating to a temperature where the system was liquid and then annealing for 3–30 days at a suitable, lower temperatures according to published or estimated phase diagrams (now available as ref 19).

The Ta containers were opened in a second glovebox with similar H_2O/O_2 removal capabilities that was equipped with a nearly horizontal window that allowed for microscopic examination of the products. Powdered samples for Guinier X-ray diffraction were mounted between the customary pieces of cellophane tape, while suitable single crystals were mounted in 0.2- or 0.3-mm thin-wall capillaries when appropriate. National Bureau of Standards Si was included with the powdered samples as an internal standard, and lattice constants of known structure types were refined therefrom by standard least-squares techniques (λ = 1.540 56 Å) with indices assigned on the basis of the pattern calculated with the aid of PWDR.[20] Plots of data from the last program were widely used to identify products of reactions. Patterns of some single-phase products were also successfully indexed by TREOR.[21]

Crystallography. The X-ray structures of six different compounds were refined in the course of this work: Sr_5Sb_3, Ca_5Sb_3Cl, Ba_5Sb_3Cl, Ca_5Sb_3F, Ca_5Bi_3F, and $Ba_4Sb_{2.5}I_{0.5}$. Data were collected at room temperature with Mo Kα radiation in all cases and on a Syntex $P2_1$ diffractometer for the two chlorides and on a Datex instrument for the other four. Crystal data and refinement pa-

(17) Garcia, E.; Corbett, J. D. *Inorg. Chem.* **1988**, *27*, 2353.
(18) Hwu, S.-J.; Corbett, J. D.; Poeppelmeier, K. R. *J. Solid State Chem.* **1985**, *57*, 43.
(19) *Binary Alloy Phase Diagrams*; American Society for Metals: Metals Park, OH 44073, 1986; Vol. 1, 2.
(20) Clark, C. M.; Smith, D. K.; Johnson, G. J. A Fortran II Program for Calculating X-Ray Diffraction Patterns—Version 5. Department of Geosciences, Pennsylvania State University, University Park, PA, 1973.
(21) Werner, P. E. TREOR-4. Trial and Error Program for Indexing Unknown Powder Patterns. Department of Structural Chemistry, Arrhenius Laboratory, University of Stockholm; 106 91 Stockholm, Sweden, 1984.

rameters are listed in Table I. All diffraction data were corrected for absorption by a ψ-scan method, as before,[18] the correction being applied as a function of θ as well by means of three scans for Sr_5Sb_3 and the two fluorides and two scans for the others.

Initial positional parameters for the first three were modeled on the Mn_5Si_3 structure type that was already known with a high degree of probability from prior powder pattern observations and successful lattice constant refinements. The presence of interstitial chloride was expected and very obvious. The two fluorides were placed in space group *Pnma* and modeled after β-Yb_5Sb_3[22] on the basis of their powder patterns, the observed systematic absences, and the lattice dimensions, and from the knowledge that the β-Yb_5Sb_3 type structure is observed for the parent Ca_5Sb_3 and Ca_5Bi_3 but with distinctly different lattice constants (vide infra). The fluoride atom in Ca_5Sb_3F was readily located in a tetrahedral hole in a difference Fourier map when $R = 0.089$. The defect anti-Th_3P_4-type model for the structure of $Ba_4Sb_{2.5}I_{0.5}$ was based on the powder pattern solution of that type provided for $Ca_4Sb_{2.4}S_{0.4}$ by TREOR[21] (see results).

The refinements were not noteworthy, and the results are generally without significant problems. The occupancies in the Sr_5Sb_3 case (with Sr1 fixed) refined to $Sr_{5.00(2)}Sb_{3.02(2)}$. The occupancies of the interstitial chlorine or fluorine in other phases were refined along with all other variables in the last few cycles, and these converged to within 10% ($\leq 1.5\sigma$) of unity in all cases (Table I). The largest residuals in the final difference Fourier maps for each phase were, in $e^-/Å^3$ as follows: Sr_5Sb_3, 0.9 both at 0,0,$^1/_4$, 2.4 Å from Sr2, and at 0,0.53,$^1/_4$, 1.3 Å from Sb; Ca_5Sb_3Cl, 1.0 only 1.3 Å from Sb; Ba_5Sb_3Cl, 1.1 very close to Ba2; Ca_5Sb_3F, 1.2 that was 0.95 Å from Sb1; Ca_5Bi_3F, ≤ 1.5 near metal atoms; $Ba_4Sb_{2.5}I_{0.5}$, ≤ 0.6. The quality of the Ca_5Bi_3F structural solution was likely limited by both a crystal of marginal quality and the natural limitations in the absorption correction achieved for a strongly absorbing crystal ($\mu = 530$ cm^{-1}) of 6:1 extreme dimensions that had to be sealed within a capillary to protect it from the atmosphere.

Results and Discussion

The results are concerned with binary phases in two structure types, the hexagonal Mn_5Si_3 (M) and the orthorhombic β-Yb_5Sb_3 type (Y), the isostructural derivatives of these that can be prepared with interstitial chloride or bromide (M) or fluoride (Y), and how these compare with literature reports. Subsequently, we will also describe different phases with the anti-Th_3P_4-type structure that are obtained with sulfide or iodide.

Binary Mn_5Si_3-Type (M) Phases. As reported before, the compounds $(Ca,Sr,Ba)_5Sb_3$ and $(Sr,Ba)_5Bi_3$ exist in this structure. The first in each group, Ca_5Sb_3 and Sr_5Bi_3, also occurs in the β-Yb_5Sb_3 (Y) structure, and samples are ordinarily obtained with both structures present. On the other hand, Ca_5Bi_3 is found only in the Y structure. All of the single-structure compounds appear to be nominally stoichiometric as they were obtained as single phases, and the A:Pn ratios of 1.67:1 used in sample preparation are thought to be accurate to about ±1%. The parameters that determine the M–Y structure distribution for the dimorphic Ca_5Sb_3 and Sr_5Bi_3 are at present unclear. Nearly pure M-Ca_5Sb_3 has been obtained by quenching samples from near 800 °C, while Y-Ca_5Sb_3 is dominant in calcium-rich samples. The molar volumes of the two are very similar (see below). The lattice parameters of all of these phases will be considered shortly in a comparison with the halide products.

A single-crystal study of one example, Sr_5Sb_3, was carried out to check the actual composition as well as the absence of disorder between lattice and interstitial sites in this structure. The positional data are listed in Table II along with those for two A_5Pn_3Cl phases to be considered later. The distances therein and a description of the structure will be given shortly. The most important feature of this result is that the atom positions are fully occupied and that the interstitial hole often occupied in this structure type (below) is empty (0.2 $e^-/Å^3$ observed). Thus this, and presumably the remainder of the binaries, do not have $A_5Pn_{3.33}$ compositions with sufficient disordered Sb or Bi interstitials to make them Zintl (valence) phases.

Table II. Refined Positional Parameters for Sr_5Sb_3, Ca_5Sb_3Cl, and Ba_5Sb_3Cl[a]

atom	x	y	z	B_{iso}, Å^2
Sr1	$^1/_3$	$^2/_3$	0	1.63 (7)
Sr2	0.2523 (1)	0	$^1/_4$	2.23 (5)
Sb	0.60979 (9)	0	$^1/_4$	1.35 (3)
Ca1	$^1/_3$	$^2/_3$	0	1.30 (2)
Ca2	0.2568 (4)	0	$^1/_4$	1.57 (2)
Sb	0.6091 (1)	0	$^1/_4$	0.94 (8)
Cl	0	0	0	1.4 (3)
Ba1	$^1/_3$	$^2/_3$	0	2.0 (1)
Ba2	0.2578 (2)	0	$^1/_4$	2.1 (1)
Sb	0.6088 (2)	0	$^1/_4$	1.7 (1)
Cl	0	0	0	2.3 (5)

[a] Space group $P6_3/mcm$; refinement data in Table I.

An unusual feature of these A_5Pn_3 phases is that they are one electron short of being Zintl (valence) phases. The valence p orbitals of antimony and bismuth can be presumed to lie well below those of the alkaline-earth-metal components in these polar intermetallics[17] so that the former will be filled first and at the expense of the more active metal. This would leave one electron (5·2 – 3·3) in a conduction band with largely A character. This last electron must become localized on addition of a halogen atom to the one interstitial site per formula unit. Such appears to be the case in many instances, with a clear size discrimination between chlorine and bromine, which bond within the M structure type, and fluorine, which takes up a four-coordinate site in the Y-type arrangement. Iodine does otherwise.

Reactions with Chlorine and Bromine. Reactions of ACl_2 with A and Pn at 850–950 °C for 1–2 weeks give A_5Pn_3Cl in evidently quantitative yields according to the stoichiometry

$$ACl_2 + 9A + 6Pn \rightarrow 2A_5Pn_3Cl$$

The lustrous, dark gray–black products all exhibit the M structure. This pertains to all systems (the Sr_5Bi_3Cl synthesis was not attempted) including Ca_5Bi_3Cl where the binary system at this proportion exhibits only the orthorhombic Y structure. Bromides behaved likewise for all systems examined, giving the corresponding $(Ca,Ba)_5(Sb,Bi)_3Br$ compounds. The lattice dimensions for all of these phases together with our and the literature parameters for the respective binary phases in the M structure are listed in Table III.

Well-determined lattice constants appear to distinguish clearly between the (empty) binary A_5Pn_3 phases and the chloride-filled ternary phases A_5Pn_3Cl as these differ generally by 0.05–0.10 Å in each dimension. On the other hand, powder pattern intensities alone are usually insufficiently different to discrimate phases with and without the chloride, although discernible intensity changes in the two lowest angle lines do occur with the lightest elements, i.e., for $Ca_5Sb_3(Cl)$. Lattice dimensions from the literature suggest that most earlier reports probably did *not* pertain to the chlorides. These conclusions are most ambiguous in the cases of Ca_5Sb_3, Sr_5Sb_3, and Sr_5Bi_3 as the reported constants deviate in opposite directions from ours (Table III). Lattice dimensions determined by either Debye–Scherrer or single-crystal diffractometer means may not

(22) Brunton, G. D.; Steinfink, H. *Inorg. Chem.* **1971**, *10*, 2301.

Table III. Lattice Dimensions (Å) of A_5P_3 and A_5P_3X Phases for A = Ca or Ba, P = Sb or Bi, X = Cl or Br, in the Mn_5Si_3 Structure (Space Group $P6_3/mcm$)

compd	*a*	*c*	*c*/*a*	method[a]	ref
Ca_5Sb_3	9.02_4	7.05_7	0.782	ds	3
Ca_5Sb_3	9.0321 (3)	7.0280 (8)	0.778	g	
Ca_5Sb_3Cl	9.0805 (3)	7.0898 (6)	0.781	g	
Ca_5Bi_3Cl[b]	9.220 (1)	7.166 (1)	0.777	g	
Ca_5Bi_3Br	9.2743 (5)	7.2832 (8)	0.785	g	
Sr_5Sb_3	9.496 (5)	7.422 (5)	0.782	d	4
Sr_5Sb_3	9.5037 (5)	7.4095 (8)	0.780	g	
Sr_5Sb_3Cl	9.5541 (4)	7.4328 (7)	0.778	g	
Sr_5Bi_3	9.63 (1)	7.63 (2)	0.792	d	5
Sr_5Bi_3	9.651 (2)	7.523 (5)	0.780	g	
Ba_5Sb_3	9.97 (1)	7.73 (2)	0.775	d	5
Ba_5Sb_3	9.964 (3)	7.694 (4)	0.772	g	
Ba_5Sb_3Cl	10.062 (4)	7.770 (6)	0.772	g	
Ba_5Sb_3Br	10.1213 (9)	7.852 (2)	0.776	g	
Ba_5Bi_3	10.10	7.78	0.770	ds	3
Ba_5Bi_3	10.13 (1)	7.79 (2)	0.769	d	5
Ba_5Bi_3	10.098 (2)	7.768 (3)	0.769	g	
Ba_5Bi_3Cl	10.188 (3)	7.837 (4)	0.769	g	
Ba_5Bi_3Br	10.251 (2)	7.918 (2)	0.772	g	

[a] d = diffractometer; ds = Debye–Scherrer powder diffraction; g = Guinier powder diffraction with Si as internal standard; λ = 1.540 56 Å (this work). [b] The binary Ca_5Bi_3 has the β-Yb_5Sb_3 structure.

Table IV. Distances (Å) in Sr_5Sb_3, Ca_5Sb_3Cl, Ba_5Sb_3Cl, and Ba_5Sb_3

atom 1–atom 2	Sr_5Sb_3	Ca_5Sb_3Cl	Ba_5Sb_3Cl	Ba_5Sb_3[a]
Sb–A2[b] (2×)	3.257 (1)	3.135 (1)	3.466 (3)	3.43
Sb–A2 (1×)	3.398 (2)	3.209 (4)	3.532 (4)	3.57
Sb–A2 (2×)	3.930 (1)	3.761 (1)	4.110 (3)	4.11
Sb–A1 (4×)	3.4708 (3)	3.327 (1)	3.662 (2)	3.63
A1–A1 (2×)	3.7048 (4)	3.556 (2)	3.885 (4)	3.87
A1–A2 (6×)	4.062 (1)	3.871 (2)	4.260 (3)	4.27
A1–Sb (6×)	3.4611 (4)	3.327 (1)	3.662 (2)	3.63
A2–A1 (4×)	4.062 (1)	3.871 (2)	4.260 (3)	4.27
A2–A2 (2×)	4.153 (2)	4.053 (7)	4.493 (5)	4.32
A2–A2 (4×)	4.413 (1)	4.257 (3)	4.672 (3)	4.60
A2–Sb (2×)	3.257 (1)	3.135 (1)	3.466 (3)	3.43
A2–Sb (1×)	3.398 (2)	3.209 (4)	3.532 (4)	3.57
A2–Sb (2×)	3.930 (1)	3.761 (2)	4.110 (3)	4.11
Cl–A2 (6×)		2.939 (3)	3.241 (2)	
Cl–Cl (2×)		3.556 (2)	3.885 (4)	
Cl–Sb (6×)		3.981 (1)	4.389 (3)	

[a] Data from ref 5. [b] A = Ca, Sr, or Ba.

be particularly accurate,[23,24] but the differences in *c* for Ca_5Sb_3 and Sr_5Bi_3 are appreciable. The *c* dimension for the former is actually closer to that of the chloride, and this was obtained for a product left (along with Sr_4Sb_2O) after leaching a Sr_4Sb composition with NH_3(l). The larger *c*/*a* ratio observed for the hexagonal product from some Ca_5Sb_3–S (and other) reactions (below) may be relevant.

The results of some brief explorations of a possible chlorine nonstoichiometry in Ca_5Sb_3Cl and Ba_5SbCl suggest any effect is small. Attempted syntheses of Ca_5Sb_3Cl samples with 25% or greater chlorine deficiencies resulted in lattice constants that were reduced only 10–15% of the way from Ca_5Sb_3Cl toward Ca_5Sb_3. The effect with Ba_5Sb_3Cl was even smaller. There was no evidence of mixed Cl–F interstitials forming in the $Ca_5Sb_3(Cl,F)$ system after annealing at 950 °C or from 920 to 620 °C.

The crystal structures of two of the new chlorides, Ca_5Sb_3Cl and Ba_5Sb_3Cl, were refined by single-crystal, X-ray methods to confirm the powder diffraction conclusions, the interstitial location, and the stoichiometry. These established that chloride fully occupies all of the

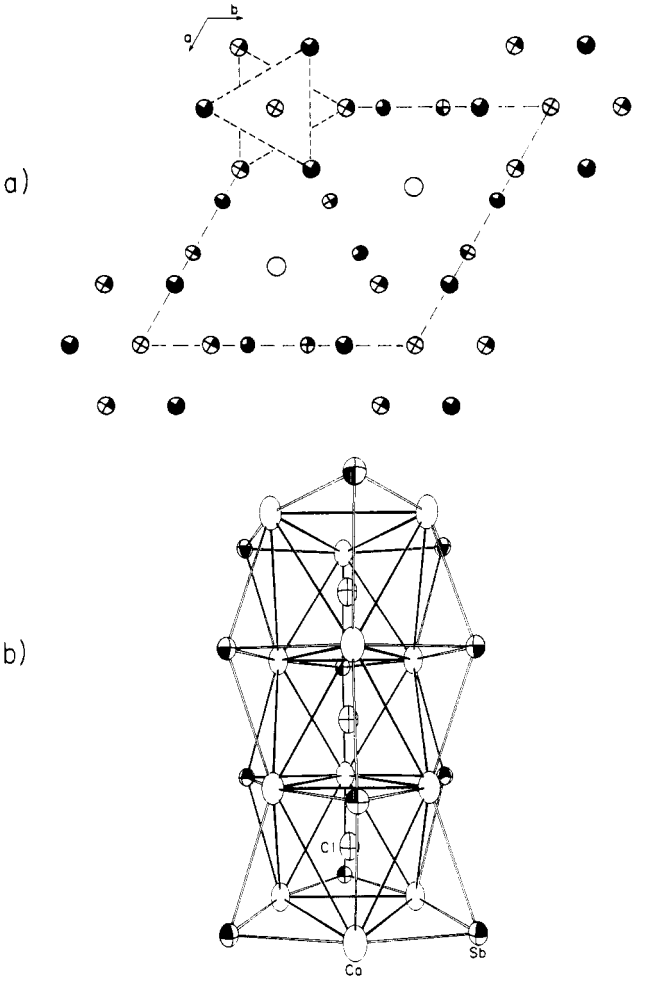

Figure 1. (a) The [001] projection of the $A_5Pn_3(Cl,Br)$ structure (Mn_5Si_3 type except for Cl, Br) with atoms shaded according to relative heights along *z*. Larger circles, A2; smaller circles, Pn; open circle, A1 at $z = 0$ and $^1/_2$; crossed circle at origin, Cl or Br at $z = 0$ and $^1/_2$. (b) An approximately [110] view of the confacial chains $^1_\infty[A_{6/2}Pn_{6/2}(Cl,Br)]$ along $\vec{c}$ with A as open ellipsoids; Pn, shaded ellipsoids; Cl or Br, crossed ellipsoid. The A polyhedra are emphasized. (Ellipsoid data from Ca_5Sb_3Cl, 90% probability.)

customary trigonal antiprismatic interstitial sites. Details are given in Tables I, II, and IV. The top of Figure 1 illustrates the hexagonal cell for the M type structure in a [001] projection in which the atoms are shaded as to height. The structure will be seen to contain infinite chains of confacial $^1_\infty[A_6Pn_6]$ trigonal antiprisms along 0,0,*z* that are, in these phases, centered by chloride, as is shown in a side view at the bottom of Figure 1. This structure also contains linear chains of A1 atoms along $^2/_3,^1/_3,z$ and $^1/_3,^2/_3,z$ with the relatively short repeat of $c/2$. These A1 atoms are in fact also bound to six of the same antimony atoms shown in the confacial chain and with only slightly greater A–Sb distances but with lower local symmetry (D_3). Figure 2 emphasizes this with a view of the environment about antimony. It should be recognized accordingly that the convenient depiction of the most interesting feature of the structure, the interstitial sites within the confacial chains shown at the bottom of Figure 1, overemphasizes the bonding anisotropy and a low dimensionality.

The chlorine–alkaline-earth metal separations in the filled structures are large compared with sum of crystal radii,[25] by 0.13 Å in the calcium compound and 0.08 Å for that with barium. Of course, these standard radii are based

(23) Taylor, R.; Kennard, O. *Acta Crystallogr.* **1986**, *B42*, 112.
(24) Jones, P. G. *Chem. Soc. Rev.* **1984**, *157*.
(25) Shannon, R. D. *Acta Crystallogr.* **1976**, *A32*, 751.

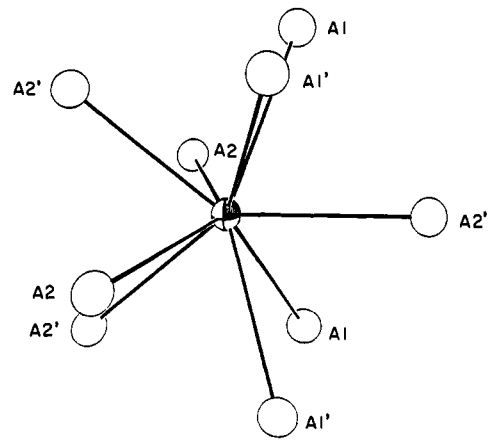

Figure 2. Alkaline-earth-metal environment about the main-group element Pn (shaded) in A_5Pn_3X (compare Figure 1a). A1 defines the linear chain along $^2/_3,^1/_3,z$, etc.; A2 is in the confacial chain. Mirror planes contain Pn and two A2 or three A2′ atoms.

mainly on data for more ionic compounds such as oxides and fluorides, while a more polar covalent interaction of the more active metal with antimony or bismuth is to be expected in the present compounds. Under these circumstances, the deviation is probably at least in the right direction.

The lattice dimension changes that occur on incorporation of interstitial halide in this structure imply an expansion of the A_6 interstitial site accompanies the process. On the other hand, the volume increments realized are relatively small compared with classical expectations. Thus cell volumes increase by only 8–10 Å^3 on bonding chlorine in the two calcium examples and by 18–20 Å^3 with the barium compounds compared with ~40 Å^3 for the standard volume of two chloride ions.[26] The Cl–Br differences are quite constant, 15–16 Å^3 vs ~10 Å^3 for standard data. Thus, a good deal of the volume necessary for the chloride already appears to be present in the host structures, as might be expected for a cavity defined by alkaline-earth-metal atoms.

Details on the anisotropic changes that occur in the cavity sizes and in the lattice dimensions on bonding of an interstitial atom have already been established many times for diverse Zr_5Sn_3Z and Zr_5Sb_3Z examples in the same structure. Here the bonding of Z is accommodated largely by expansion of just the shared faces of the Zr_6 antiprisms.[10,11] One reason for this may be the strong bonding provided by the linear Zr1 chain parallel to *c*. The only case we can directly compare for the $A_5Pn_3(Cl)$ systems is that of Ba_5Sb_3Cl with Ba_5Sb_3 where a limited refinement for the binary has been reported (isotropic temperature factors, no absorption correction, no σ's reported, R = 10.3%).[5] Within this limitation, a 0.17-Å expansion of d(Ba–Ba) in the shared faces of the trigonal antiprisms and 0.07-Å increase in d(Ba–Ba) between these appears to occur. Although one electron in the A_5Pn_3 parent phase is presumably delocalized in an A-rich conduction band, the product is a valence phase, and direct bonding along the A1 chain in the product is presumably no longer a factor. Examination of overlap (COOP) populations would be desirable so as to estimate this and other metal–metal bonding components, but none is apt to be very substantial.

That these A_5Pn_3 compounds do indeed undergo the implied metal–semiconductor transition on oxidation to the A_5Pn_3X valence phases is presently under investigation. In the Zr_5Sb_3Z systems, which are much electron-richer (11 rather than 1 electrons remaining in the empty phase), the oxidation accompanying insertion of an interstitial such as iron or sulfur results in substantial reduction of direct Zr–Zr overlap population in the antiprism portion, while those in the linear chain (large) and between the two types of zirconium chains (small) remain about constant.[10] This merely means that states associated with the latter two lie low in a rather large, metal-based conduction band. However, the approximate distance changes noted above suggest that bonding alterations in these A_5Pn_3 phases on interstitial incorporation are again largely concentrated in the interstitial cavity where (weak) A–A bonding is replaced by A–X interactions.

The availability of only one electron per formula (and structural) unit A_5Pn_3 puts a strict limit on the electron capacities of various oxidants that may be bound in the cavity, presuming that the usual valence electronic requirements of the added element and the pnictide are to be met and all interstitial sites are to be filled. Fractional occupation of this site in diverse examples of the M structure seems to be rare (but not unknown),[10,11,17] and in the present case oxide and sulfide give other structures (below). There is presumably no such electronic restriction on the amount of halide that may be bound within numerous, electron-richer examples of the Mn_5Si_3-type structure, but there is a clear limitation on cavity sizes available. Thus, it is not surprising that reactions of the analogous $Ce_5(Sb,Bi)_3$ phases, which presumably have (at least) six electrons available beyond the valence requirements of the antimony or bismuth, readily yield the corresponding Ce_5Sb_3Cl, Ce_5Bi_3Cl, and Ce_5Bi_3Br in the same structure type.[27]

Reactions with Fluorine. The β-Yb_5Sb_3 (Y) Structure. An important factor in the choice between the M (Mn_5Si_3) and Y (β-Yb_5Sb_3) structure types for the binary A_5Pn_3 phases appears to be size proportions. Thus a relatively small alkaline-earth element with bismuth affords only the Y form in Ca_5Bi_3, while Ca_5Sb_3 and Sr_5Bi_3 are dimorphic, and all of the rest (including the arsenides) have M-type structures. The larger chloride and bromide preferentially occupy the large "octahedral" sites in M-type A_5Pn_3, and this happens even with Ca_5Bi_3 where the alternative Y form is the stable binary phase. On the other hand, the smaller fluoride is well bound at least in the calcium compounds in an analogous "preformed" cavity already present in the more complex Y structure.

The reaction conditions required to make the fluoride phases seem to be significantly more severe than necessary with the heavier halides. Initially, Ca, Sb, and CaF_2 in the proper proportions were reacted at 900 °C, but this gave only CaF_2 plus the usual binary product (Y plus M structures). On the other hand, the CaF_2 disappeared when the reaction was repeated with induction heating of the components for a couple of hours at ~1250 °C followed by an annealing at 850 °C to provide better crystal development. Noticeable changes in the dimensions of the sole Y-type product were evident. A similar, apparently quantitative reaction produced Ca_5Bi_3F. On the other hand, a comparable reaction designed to synthesize Ba_5Sb_3F did not afford significant BaF_2 uptake. Lattice dimensions of the binary and ternary products in the Y-type structure together with literature data on the former are given in Table V. The incorporation of fluoride charac-

(26) Biltz, W. *Raumchemie der festern Stoffe*; Leopold Voss Verlag: Leipzig, Germany, 1934.

(27) The lattice constants are as follows: Ce_5Sb_3Cl: a = 9.4416 (9) Å, c = 6.568 (4) Å; Ce_5Bi_3Cl: a = 9.5812 (5) Å, c = 6.6334 (6) Å; Ce_5Bi_3Br: a = 9.6252 (5) Å, c = 6.6974 (6) Å, all in $P6_3/mcm$.

Table V. Lattice Constants of A_5Pn_3 and A_5Pn_3F Phases with the β-Yb_5Sb_3 Structure[a]

compd	a, Å	b, Å	c, Å	V, Å^3	method[b]	ref
Ca_5Sb_3	12.502 (8)	9.512 (7)	8.287 (7)		d	6
Ca_5Sb_3	12.537 (4)	9.555 (2)	8.296 (2)	993.8 (5)	g	
Ca_5Sb_3F	12.442 (2)	9.653 (2)	8.381 (2)	1006.6 (3)	g	
Ca_5Bi_3	12.722 (8)	9.666 (6)	8.432 (6)		d	7
Ca_5Bi_3	12.766 (1)	9.706 (2)	8.437 (2)	1045.3 (3)	g	
Ca_5Bi_3F	12.602 (2)	9.771 (2)	8.501 (2)	1046.8 (3)	g	
Sr_5Bi_3	12.37_0	10.23_3	8.89_0		ds	3

[a] Y-type, space group *Pnma*. [b] d = diffractometer; ds = Debye–Scherrer powder diffraction; g = Guinier powder diffraction with Si as internal standard; λ = 1.540 56 Å (this work).

Table VI. Positional Parameters for Ca_5Sb_3F and Ca_5Bi_5F (β-Yb_5Sb_3 Type)

atom	x	y	z	B_{iso}, Å^2
Sb1	−0.01841 (4)	$^1/_4$	0.41771 (5)	1.16 (2)
Sb2	0.17037 (3)	−0.01878 (4)	0.07525 (4)	1.32 (2)
Ca1	0.07273 (9)	0.0422 (1)	0.6933 (1)	1.54 (4)
Ca2	0.2290 (1)	$^1/_4$	0.3229 (2)	1.59 (6)
Ca3	0.0074 (1)	$^1/_4$	0.0444 (2)	1.37 (5)
Ca4	0.2855 (1)	$^1/_4$	0.8561 (2)	1.59 (6)
F[b]	0.1036 (3)	$^1/_4$	0.8029 (5)	1.3 (2)
Bi1	−0.0188 (1)	$^1/_4$	0.4171 (2)	1.16 (5)
Bi2	0.17092 (7)	−0.01882 (8)	0.0766 (1)	1.28 (3)
Ca1	0.0722 (4)	0.0443 (4)	0.6939 (6)	1.5 (2)
Ca2	0.2300 (6)	$^1/_4$	0.3209 (8)	1.5 (3)
Ca3	0.0077 (6)	$^1/_4$	0.0317 (9)	1.4 (3)
Ca4	0.2835 (6)	$^1/_4$	0.8583 (9)	1.5 (3)
F[c]	0.105 (2)	$^1/_4$	0.803 (3)	1.7 (3)

[a] Atoms numbered as in the parent structure type[22] but with the origin shifted $0,0,^1/_2$ to allow closer comparison with the Y_5Bi_3-type structure.[17,29] [b] Refined occupancy = 1.01 (1). [c] Refined occupancy = 0.98 (5).

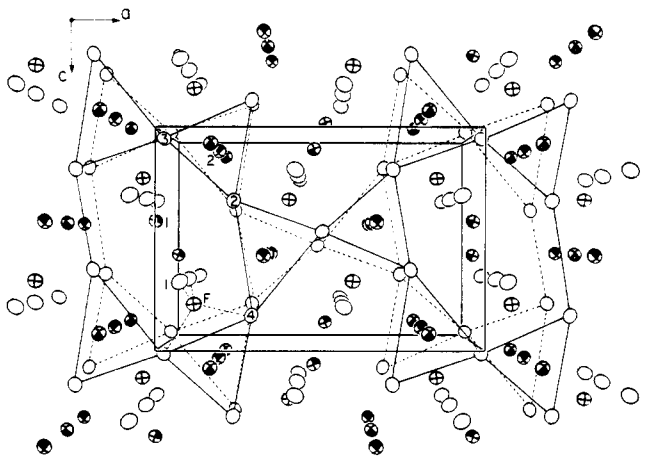

Figure 3. A [010] perspective of the structure of Ca_5Sb_3F (β-Yb_5Sb_3 type except for F) with the atom numbering scheme. Calcium (open ellipsoids) defines layers at $y = ^1/_4$ and $^3/_4$, which are outlined by dashed and solid lines, respectively. Antimony ellipsoids are shaded and fluorine, crossed. The approximately tetrahedral arrangement of calcium about fluorine is shown with dotted lines at the lower left (50% ellipsoids).

teristically reduces the *a* and increases the *b* and *c* dimensions of the orthorhombic cell by significant amounts.

Single-crystal X-ray methods were used to define the structures of both Ca_5Sb_3F and Ca_5Bi_3F. The refined positional data are given in Table VI, and some significant distances in Table VII. The fluorine in each effectively refines to full occupancy (Table I).

The structure is illustrated in Figure 3 for Ca_5Sb_3F. It can be described in terms of very similar (but not superimposed) layers of alkaline-earth-metal atoms at $y = ^1/_4$ and $^3/_4$ (open ellipsoids) that are related by glide planes normal to $\vec{a}$ and $\vec{c}$ (or by inversion through $^1/_2,^1/_2,^1/_2$). The

Table VII. Distances[a] (Å) and Angles (deg) about Fluorine in Ca_5Sb_3F and Ca_5Bi_3F

atom 1–atom 2	Ca_5Sb_3F	Ca_5Bi_3F
Ca1–Pn1[b] (×1)	3.042 (1)	3.100 (4)
Ca1–Pn1 (×1)	3.259 (1)	3.300 (5)
Ca1–Pn2 (×1)	3.345 (1)	3.396 (6)
Ca1–Pn2 (×1)	3.471 (1)	3.537 (5)
Ca1–Pn2 (×1)	3.593 (1)	3.641 (5)
Ca1–Ca3 (×1)	3.582 (2)	3.599 (8)
Ca1–Ca4 (×1)	3.584 (2)	3.617 (8)
Ca1–Ca3 (×1)	3.759 (2)	3.837 (7)
Ca1–Ca1 (×1)	3.795 (2)	3.864 (10)
Ca1–Ca2 (×1)	3.895 (2)	3.955 (7)
Ca1–Ca1 (×1)	4.007 (2)	4.021 (8)
Ca2–Pn1 (×1)	3.171 (2)	3.240 (8)
Ca2–Pn2 (×2)	3.316 (1)	3.374 (5)
Ca2–Pn2 (×2)	3.398 (1)	3.430 (5)
Ca2–Pn1 (×1)	3.727 (2)	3.758 (8)
Ca2–Ca3 (×1)	3.656 (2)	3.718 (11)
Ca2–Ca3 (×1)	3.661 (2)	3.727 (10)
Ca2–Ca1 (×2)	3.895 (2)	3.955 (7)
Ca2–Ca4 (×1)	3.973 (2)	3.990 (10)
Ca3–Pn1 (×1)	3.226 (2)	3.293 (8)
Ca3–Pn1 (×2)	3.268 (1)	3.320 (5)
Ca3–Pn2 (×2)	3.305 (1)	3.358 (4)
Ca3–Ca1 (×2)	3.582 (2)	3.599 (8)
Ca3–Ca2 (×1)	3.656 (2)	3.718 (11)
Ca3–Ca2 (×1)	3.661 (2)	3.727 (10)
Ca3–Ca1 (×2)	3.759 (2)	3.837 (7)
Ca3–Ca4 (×1)	3.761 (2)	3.775 (10)
Ca4–Pn1 (×1)	3.084 (2)	3.140 (8)
Ca4–Pn1 (×2)	3.286 (1)	3.342 (6)
Ca4–Pn2 (×2)	3.483 (1)	3.515 (5)
Ca4–Ca1 (×2)	3.584 (2)	3.617 (8)
Ca4–Ca3 (×1)	3.761 (2)	3.775 (10)
Ca4–Ca2 (×1)	3.973 (2)	3.990 (10)
Pn1–Ca1 (×2)	3.042 (1)	3.100 (4)
Pn1–Ca4 (×1)	3.084 (2)	3.140 (8)
Pn1–Ca2 (×1)	3.171 (2)	3.240 (8)
Pn1–Ca1 (×2)	3.226 (2)	3.300 (5)
Pn1–Ca3 (×1)	3.259 (1)	3.293 (8)
Pn1–Ca2 (×1)	3.727 (2)	3.758 (8)
Pn2–Ca3 (×1)	3.268 (1)	3.320 (5)
Pn2–Ca3 (×1)	3.286 (1)	3.358 (6)
Pn2–Ca2 (×1)	3.305 (1)	3.379 (4)
Pn2–Ca4 (×1)	3.316 (1)	3.342 (6)
Pn2–Ca1 (×1)	3.345 (1)	3.396 (6)
Pn2–Ca2 (×1)	3.398 (1)	3.430 (5)
Pn2–Ca1 (×1)	3.471 (1)	3.537 (5)
Pn2–Ca4 (×1)	3.483 (1)	3.515 (5)
Pn2–Ca1 (×1)	3.593 (1)	3.641 (5)
F–Ca1 (×2)	2.237 (2)	2.25 (1)
F–Ca3 (×1)	2.276 (5)	2.30 (2)
F–Ca4 (×1)	2.301 (5)	2.29 (3)
F–Pn2 (×2)	3.550 (3)	3.61 (1)
F–Pn1 (×1)	3.564 (4)	3.63 (2)
F–Pn2 (×2)	4.059 (4)	4.09 (2)
	Angles about F	
Ca1–Ca1	127.2 (2)	
Ca1–Ca4	104.3 (1)	
Ca1–Ca3	105.0 (1)	
Ca3–Ca4	110.5 (2)	

[a] Distances < 4.1 Å. [b] Pn = Sb or Bi.

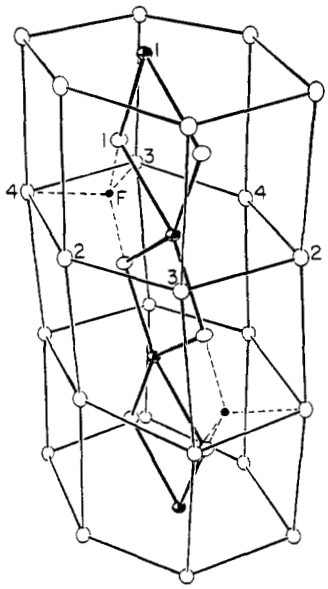

Figure 4. Approximately hexagonal channel of calcium atoms along $0,y,{}^1/_2$ in Ca_5Sb_3F (Figure 3) with the b axis oriented vertically. Contained atoms are Ca1 (open circles), Sb1 (shaded), and F(solid) (90% probability).

more distant layer is defined by dashed lines in the figure. The two layers define nominal trigonal prisms that are interconnected by sharing all edges along $\vec{b}$, and each is centered by an Sb2 atom near $y = {}^1/_2$ (or 0). Of course, this array is infinite along $\vec{b}$ as well with the trigonal prisms sharing opposite triangular faces. Large hexagonal channels around $0,y,{}^1/_2$ that are generated by the array of condensed prisms contain two additional Ca1 atoms (per cell) near $y = 0, {}^1/_2$ and two Sb1 atoms at $y = {}^1/_4, {}^3/_4$.[28] Finally, fluorine occupies two approximately tetrahedral sites surrounded by calcium at opposite ends of this (former) channel. Dotted lines have been added in the lower left of Figure 3 to connect one fluorine to the four neighboring calcium atoms. The structure within these hexagonal tunnels and the position of interstitial fluorine is better seen in the view given in Figure 4. Very similar cavities were of course already present in the parent binary phase.

The Ca_4F unit in Ca_5Sb_3F is illustrated in Figure 5. It is interesting to note that all four of fluorine's neighbors, Ca1(×2),3,4, are five-coordinate to Sb or Bi, while the fourth, Ca2, is six-coordinate by only Pn. One angle of the nominal tetrahedron, Ca1–F–Ca1, is relatively large, 127.2°. The average Ca–F distance is, in contrast to the trend noted above with the chloride, 0.05 Å shorter than the sum of crystal radii using the value for six-coordinate calcium.[25] (The experimental value for CaF_2, 2.366 Å, is similarly 0.06 Å less than the sum of standard data for eight-coordinate metal.) The empty cavity in Y-Ca_5Sb_3[6] into which fluorine becomes bound appears to have undergone a small expansion in the process, and a tightness of the fit may be reflected the perhaps small value of $\bar{d}$(Ca–F). A striking counter change on fluorine incorporation is the 0.09 Å decrease in the Ca3–Ca4 edge of this polyhedron. With Ca_5Bi_3F this contraction from that in the binary phase[7] stands out even more, 0.17 Å compared with only ~0.03 Å changes in all other of the shorter Ca–Ca distances. Both

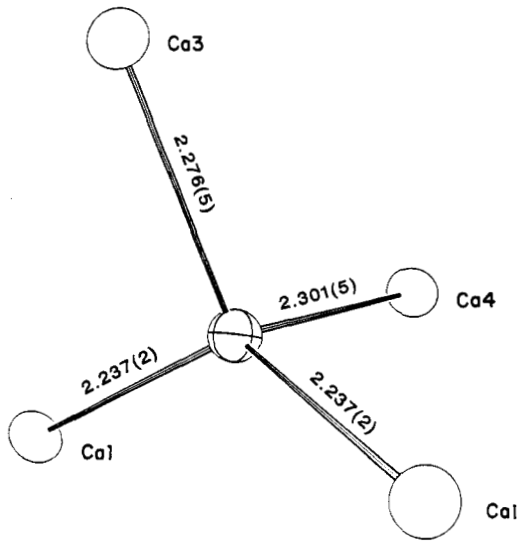

Figure 5. Fluorine environment in Ca_5Sb_3F.

decreases parallel the distinctive decrease seen only in the a lattice dimension on formation of this phase (Table V), consistent with the relative orientation of the Ca3–Ca4 separation (Figure 3). Our inability to make the corresponding Ba_5Sb_3F may well be a simple consequence of an oversized tetrahedral cavity in Ba_5Sb_3.

Further comparison of the distances found here with those reported for Ca_5Sb_3 does not seem worthwhile as most differences are fairly small. The literature values for a and b lattice dimensions of Y-type Ca_5Sb_3 and Ca_5Bi_3 are distinctly less than ours, but the differences are not suggestive of a fluoride pressure. Error estimates for distances in both Ca_5Bi_3[7] and Ca_5Bi_3F are sufficiently large (probably originating with the severe X-ray absorption problem) that most perceived differences are not apt to be significant.

We also sought to check the parent β-Yb_5Sb_3[22] in the unlikely circumstance that that phase had also contained fluorine, but we instead found a problem with stoichiometry. Single phase M-(α-)Yb_5Sb_3 was again obtained on quenching the stoichiometric reaction from ~1300 °C, and its lattice dimensions (a = 9.0344 (2), b = 6.9112 (4) Å) were each about 0.04 Å larger than reported before.[30] This phase on annealing for 3 weeks at 800 or 900 °C again transformed into Y-(β-)Yb_5Sb_3 *and* Yb_4Sb_3 (anti-Th_3P_4). These observations clearly present a stoichiometric puzzle even if allowance is made for the fact that the Yb_4Sb_3 probably has a defect structure and is closer to the composition Yb_3Sb_2 (=$Yb_4Sb_{2.67}$), like Eu_3As_2.[14,31] The M-form of Yb_5Sb_3 as isolated could be antimony-richer, akin to Zr_5Sb_{3+x}[17] and others, but that does not seem likely for our sample. Otherwise, the Y (β) form of Yb_5Sb_3 must have an unrecognized excess of metal or a deficiency of antimony, contrary to previous conclusions.[22] Considerations of Y_5Bi_3, which has a closely related structure,[28,29] both oppose[32] and support[33] such a stoichiometric deviation for the yttrium phase.

The product of the reacton of iodine with A_5Pn_3 phases is different from those with the other halogens. The

(28) The very slightly different Y_5Bi_3 structure occurs in the same space group as β-Yb_5Sb_3 but with the a and c axes interchanged.[29] These two differ largely in the character of the buckling of the layers around $\gamma = 0, {}^1/_2$ that are defined by the A1 and Pn2 atoms.[17] The two types generally cannot be distinguished by powder patterns.

(29) Wang, Y.; Gabe, E. J.; Calvert, L. D.; Taylor, J. B. *Acta Crystallogr.* **1976**, *B32*, 1440.
(30) Bodner, R. E.; Steinfink, H. *Inorg. Chem.* **1967**, *6*, 327.
(31) Hulliger, F.; Vogt, O. *Solid State Commun.* **1970**, *8*, 771.
(32) Schmidt, F. A.; McMasters, O. D.; Lichtenberg, R. R. *J. Less-Common Met.* **1969**, *18*, 215.
(33) Yoshihara, K.; Taylor, J. B.; Calvert, L. D.; DesPault, J. G. *J. Less-Common Met.* **1975**, *41*, 329.

Table VIII. Observed and Calculated[a] Powder Patterns for $Ca_4Sb_{2.4}S_{0.4}$[a]

h k l	d_{obsd}	d_{calcd}	I_{obsd}	I_{calcd}
2 1 1	3.941 (4)	3.9399	50	42
2 2 0	3.413 (3)	3.4121	2	1
3 1 0	3.052 (3)	3.0519	100	100
3 2 1	2.579 (2)	2.5793	60	62
4 0 0	2.413 (2)	2.4127	2	1
4 2 0	2.158 (1)	2.1580	35	29
3 3 2	2.058 (1)	2.0576	25	19
4 2 2	1.970 (1)	1.9700	10	10
4 3 1, 5 1 0	1.8930 (9)	1.8923	30	22
5 2 1	1.7621 (8)	1.7620	10	5
4 4 0	1.7060 (7)	1.7060	2	2
5 3 2, 6 1 1	1.5656 (6)	1.5656	40	36
6 2 0	1.5259 (6)	1.5259	20	19
5 4 1	1.4894 (5)	1.4892	20	15
6 3 1	1.4227 (5)	1.4229	2	4
4 4 4	1.3927 (4)	1.3930	10	8
5 4 3		1.3648		1
6 4 0	1.3385 (4)	1.3383	15	8
7 2 1, 6 3 3, 5 5 2	1.3133 (4)	1.3133	40	31
6 4 2	1.2895 (4)	1.2896	5	6
7 3 0	1.2668 (4)	1.2672	2	1
6 5 1, 7 3 2	1.2257 (3)	1.2257	10	6
8 0 0	1.2065 (3)	1.2064	2	1
6 5 3	1.1535 (3)	1.1535	10	7
8 2 2	1.1370 (3)	1.1374	2	3
7 4 3, 7 5 0, 8 3 1	1.1219 (3)	1.1219	20	16
7 5 2	1.0930 (2)	1.0927	5	6

[a] Anti-Th_3P_4 structure, space group $I\bar{4}3d$, a = 9.6508 (3) Å, x(Ca) = 0.083, Cu Kα radiation, λ = 1.54056 Å.

identification of the iodine result will be clearer after the course of the reaction of sulfur with Ca_5Sb_3 is described (below).

Reactions with Carbon and Oxygen. If we are correct in the characterization of these hosts and their reactions, the present A_5Pn_3 phases might react with carbon and oxygen to produce Zintl phases $A_5Pn_3C_{0.25}$ and $A_5Pn_3O_{0.5}$, respectively, in which the interstitials are either disordered or ordered in some superstructure. However, postulates of this sort suffer from a substantial limitation, the absence of any consideration of the stability of alternate phases that contain the carbon or oxygen. In fact, the reactions with carbon and oxygen for the example of Ca_5Sb_3 proceed at 870–900 °C as

$$5Ca + 3Sb + C \rightarrow \tfrac{1}{2}CaC_2 + \tfrac{3}{2}\text{"}Ca_3Sb_2\text{"}$$

$$4Ca + 3Sb + CaO \rightarrow Ca_4Sb_2O + \tfrac{1}{11}Ca_{11}Sb_{10} (+\tfrac{1}{11}Sb)$$

The composition of the new product in the first reaction is only approximately Ca_3Sb_2; this phase will be the subject of a later report.[34] The Ca_4Sb_2O and $Ca_{11}Sb_{10}$ products from the second were identified with the aid of patterns calculated for the known structures,[13,35] but the state of the small amount of antimony that should have been left in the second reaction was not identified. Reaction with half as much CaO gave Ca_4Sb_2O and "Ca_3Sb_2".

Reaction with Sulfur. The proportions necessary to produce $Ca_5Sb_3S_{0.5}$ gave a chunklike dark gray product with some luster following 870 °C for 5 days and annealing at 640 °C for 4 days. The powder pattern was complex and completely different from that of any phase described heretofore. Fortunately, all 19 lines with $I/I(\max) \geq 0.05$ could be indexed by TREOR[21] with a body-centered-cubic cell, a = 9.6508 (3) Å. Consideration of the systematic absences and the literature led us to the conclusion that the compound was $Ca_4Sb_{2.4}S_{0.4}$ (which, coincidentally, has the same composition as $Ca_5Sb_3S_{0.5}$) and that it exhibited a defect version of the anti-Th_3P_4 structure. The observed pattern, Table VIII, is very well described by that calculated by using the ideal x(Ca) parameter. Since extra lines evidencing a supercell and ordering of the nonmetals were not seen in powder patterns of the samples prepared under these particular conditions, the antimony and sulfur are presumbed to be effectively disordered over 93% (2.8/3.0) of the thorium positions. This structure represents a complex sharing of polyhedra such that the Sb/S atoms are surrounded by eight equidistant calcium atoms in an octaverticon (a strongly distorted cube) while calcium again has six Sb/S neighbors (neglecting vacancies) in the form of distorted octahedron. A defect, anti-Th_3P_4 structure for a valence compound $Ca_4(Sb_{2.4}S_{0.4})$ has some precedence in the binary, semiconducting Eu_3P_2, Eu_3As_2,[31] Ba_3P_2, and Sr_3P_2,[36] all of which are better written as $A_4Pn_{2.67}$ with 11% vacancies in the latter site. (Lattice constants for Eu_3As_2 as a function of composition suggest some nonstoichiometry, however.[14]) A reaction under the same conditions designed to produce $Ba_4Sb_{2.4}S_{0.4}$ was unsuccessful.

Since the $Ca_4Sb_{2.4}S_{0.4}$ exhibits a defect structure with 7% vacancies on the latter site, some attention was given to the question as to whether a range of stoichiometries might be possible within a series of Zintl phases. The two extremes are Ca_4Sb_2S with no vacancies and $Ca_4Sb_{8/3}$ (= Ca_3Sb_2) with 11%. The former might be related to Ca_4Sb_2O in the K_2NiF_4 structure[13] while the latter has been shown to have a different structure.[34] However, the reaction with the higher sulfur proportions necessary to form the hypothetical Ca_4Sb_2S (900 °C for 19 days plus annealing at 750 and 550 °C) gave only CaS (NaCl type) plus a hexagonal M-type phase with a = 9.044 (1), c = 7.170 (3) Å (c/a = 0.793). The a value is intermediate between those for Ca_5Sb_3 and Ca_5Sb_3Cl (Table III), while the c dimension is larger than that for either. One explanation is that fractional sulfur (or antimony) interstitials may be involved, or better, that a distorted version of the structure type known as Ca_5Pb_3[37] is formed since both this and the related Eu_5As_3[14] exhibit a larger c/a ratio. This last type of structure, which generally cannot be distinguished from M-type by its powder pattern alone, is under further study.

Table IX. Refined Positional and Thermal Parameters of $Ba_4Sb_{2.5}I_{0.5}$[a]

atom	posn	x	y	z	B_{11}[b]	B_{22}	B_{12}
Ba	16c	0.0713 (2)	x	x	2.2 (1)	B_{11}	0.16 (8)
Sb, I	12a[c]	$^3/_8$	0	$^1/_4$	2.1 (3)	1.6 (2)	0

[a] Space group $I\bar{4}3d$. [b] $B_{22} = B_{33}$ and $B_{12} = B_{13} = B_{23}$. [c] The position was refined as $^5/_6$Sb, $^1/_6$I.

Reaction with Iodine. A sample reaction to produce Ba_5Sb_3I was run at 870 °C for 6 days followed by successive annealing at 770, 670, and 470 °C. The powder pattern could not be indexed and was concluded to be that of a mixture. The reaction process was subsequently established to be

$$30Ba + 16Sb + 2SbI_3 \rightarrow 6Ba_4Sb_{2.5}I_{0.5} + 3Ba_2SbI$$

on the basis of the identification of the first product by single-crystal means and of the second by subsequent considerations of stoichiometry and of the literature followed by a powder pattern calculation. The former was then also synthesized directly.

The X-ray structure of a single crystal of what turned out to be $Ba_4Sb_{2.5}I_{0.5}$ was originally studied with a primitive

(34) Hurng, W.-M.; Corbett, J. D., unpublished research.
(35) Deller, K.; Eisenmann, B. *Z. Naturforsch.* **1976**, *31b*, 29.
(36) Maass, K. E. *Z. Anorg. Allg. Chem.* **1970**, *374*, 11, 19.
(37) Helleis, O.; Kandler, H.; Leicht, E.; Quiring, W.; Wolfel, E. *Z. Anorg. Allg. Chem.* **1963**, *320*, 86.

Table X. Comparisons of the Observed and Calculated Powder Patterns of Ba_2SbI

h k l	d_{calcd}[a]	d_{obsd}	I_{calcd}[a]	I_{obsd}
2 0 0	3.549	3.547 (4)	100	100
2 2 0	2.509	2.508 (4)	79	70
2 2 2	2.049	2.042 (3)	30	20[b]
4 0 0	1.774	1.774 (3)	15	20
4 2 0	1.587	1.586 (3)	44	50
4 2 2	1.449	1.449 (3)	34	20
4 4 0	1.255	1.253 (2)	12	

[a] NaCl type. Reflections with I_{calcd} <5.0 are not listed. [b] The reflection is superimposed by one from $Ba_4Sb_{2.5}I_{0.5}$.

hexagonal setting, but without success. Consideration of the $Ca_4Sb_{2.4}S_{0.4}$ structural result and of this data set in the alternative cubic setting led to the identification and solution of the structure as $Ba_4Sb_{2.5}I_{0.5}$, again an anti-Th_3P_4 type but this time with lattice sites fully occupied. Refinement data are reported in Tables I and IX. The Ba–Sb/I distances are comparable to the shortest Ba–Sb values found in Ba_5Sb_3Cl (Table IV). Any ordering of the antimony and iodine atoms would not be expected to be discernible because of their similar scattering abilities. The literature notes that $Ba_4P_{2.5}I_{0.5}$ also adopts this structure.[38] An attempt to synthesize the analogous $Ba_4Bi_{2.5}I_{0.5}$ did not succeed.

The evident stoichiometry of the second product in the reaction above is Ba_2SbI, but the powder data were not those for the anti-α-$NaFeO_2$ type identified for Ba_2PI.[38] However, the relatively simple pattern could be fit to a NaCl-type lattice with a = 7.0970 (6) Å, and the pattern calculated on this basis have a good description of the observed one (Table X). A NaCl structure is found for a number of alkaline-earth-metal compounds of this charge type when the disordered anions are of similar size; for example, Ca_2AsBr, (which is single phase to $Ca_{2.5}AsBr_2$), Sr_2AsCl,[39] and (Ca,Sr)PCl,[40] but this is the first iodide to be so classified. The corresponding calcium iodides[41] and $Ba_2P(Cl,Br,I)$[38] have been reported only in the alternative α-$NaFeO_2$ structure.

Overview. The A_5Pn_3 compounds formed between the alkaline-earth metals and the pnictides As, Sb, or Bi appear to be stoichiometric, and they occur in either an Mn_5Si_3 (M) or a β-Yb_5Sb_3 (Y) structure. These all have one excess valence electron and are probably, but not assuredly, metallic. Each structure type contains suitable interstitial sites so that isostructural A_5Pn_3X phases, Pn = Sb, Bi, can be obtained with X = Cl, Br in the former as well as Ca_5Pn_3F phases in the latter structure type. The larger sized iodide or the smaller amount of sulfide necessary for a valence phase are accommodated in the alternative Zintl phases $Ba_4Sb_{2.5}I_{0.5}$ and $Ca_4Sb_{2.4}S_{0.4}$ for the two A_5Pn_3 systems studied. Both have an anti-Th_3P_4 type structure. Oxide produces the already known Zintl phase Ca_4Sb_2O (K_2NiF_4 type),[13] while carbon appears to be most stable as CaC_2.

Phases with the M structure that have greater numbers of excess valence electrons such as Zr_5Sb_3 and Zr_5Sn_3 also form comparable interstitial structures but without as great a restriction on the valence characteristics of the interstitial.[10,11] Explorations with halogen in rare-earth-metal analogues show that M-type $Ce_5(Sb,Bi)_3(Cl,Br)$ phases readily form as well. A field rich in new materials appears possible here. Quantification of other physical properties and the exploration of other systems are underway.

Acknowledgment. Larry Wolfe provided equilibration data for several of the binary systems in clarification of the phase relationships. We are indebted to R. A. Jacobson for the provision of diffraction and computing facilities.

Supplementary Material Available: Tables of anisotropic thermal parameters for Sr_5Sb_3, Ca_5Sb_3Cl, Ba_5Sb_3Cl, Ca_5Sb_3F, Ca_5Bi_3F (2 pages); listings of observed and calculated structure factors for the same phases and $Ba_4Sb_{2.5}I_{0.5}$ (12 pages). Ordering information is given on any current masthead page.

(38) Hadenfeldt, C. *Z. Anorg. Allg. Chem.* **1977**, *436*, 113.
(39) Hadenfeldt, C. *Z. Naturforsch.* **1976**, *31b*, 408.
(40) Hadenfeldt, C. *Z. Naturforsch.* **1975**, *30b*, 165.
(41) Hadenfeldt, C. Herdejurgen, H. *Z. Anorg. Allg. Chem.* **1988**, *558*, 35.

Synthesis and Oxygen Reactive Ion Etching of Novolac–Siloxane Block Copolymers

M. J. Jurek,*,† R. G. Tarascon, and E. Reichmanis*

AT&T Bell Laboratories, Murray Hill, New Jersey 07974

Received December 22, 1988

The coupling reaction between dimethylamine-terminated poly(dimethylsiloxane) (PDMSX) oligomers and the phenolic hydroxyl groups of novolac resins results in block copolymer systems. The charge ratio of PDMSX oligomers will control the silicon content of the final material, which determines the solubility and O_2 reactive ion etching (RIE) resistance. Three different copolymers were prepared by using *o*-cresol and 2-methylresorcinol novolacs and poly(hydroxystyrene) as the phenolic component. At ~12 wt % silicon content these copolymers exhibited a good O_2 RIE selectivity with respect to hard-baked HPR-206 of ~1:12, which is adequate for a dry pattern transfer process. These copolymers have potential use as positive bilevel resists because of their solubility in aqueous base developers.

Introduction

Positive photoresists based on novolac resin/diazonaphthoquinone sensitizer systems have been extensively utilized due to their desirable combination of availability and materials properties,[1] such as lithographic sensitivity and aqueous base solubility. Unfortunately, their lack of

† Current address: Ciba-geigy Corp., Ardsley, NY.

(1) Willson, C. G. In *Introduction Microlithography*; Thompson, L. F., Willson, C. G., Bowden, M. J., Eds.; ACS Symposium Series No. 219; American Chemical Society: Washington, DC, 1983; p 87.

0897-4756/89/2801-0319$01.50/0